AIP Applied Physics Letters

Shape control via surface reconstruction kinetics of droplet epitaxy nanostructures

C. Somaschini, S. Bietti, N. Koguchi, and S. Sanguinetti

Citation: Appl. Phys. Lett. **97**, 203109 (2010); doi: 10.1063/1.3511283
View online: http://dx.doi.org/10.1063/1.3511283
View Table of Contents: http://apl.aip.org/resource/1/APPLAB/v97/i20
Published by the American Institute of Physics.

Related Articles

In situ study of self-assembled GaN nanowires nucleation on Si(111) by plasma-assisted molecular beam epitaxy
Appl. Phys. Lett. 100, 212107 (2012)

A master-equation approach to simulate kinetic traps during directed self-assembly
J. Chem. Phys. 136, 184109 (2012)

Physics of shell assembly: Line tension, hole implosion, and closure catastrophe
J. Chem. Phys. 136, 184507 (2012)

Evolution of self-assembled type-II ZnTe/ZnSe nanostructures: Structural and electronic properties
J. Appl. Phys. 111, 093524 (2012)

Stochastic processes in light-assisted nanoparticle formation
Appl. Phys. Lett. 100, 193106 (2012)

Additional information on Appl. Phys. Lett.

Journal Homepage: http://apl.aip.org/
Journal Information: http://apl.aip.org/about/about_the_journal
Top downloads: http://apl.aip.org/features/most_downloaded
Information for Authors: http://apl.aip.org/authors

ADVERTISEMENT

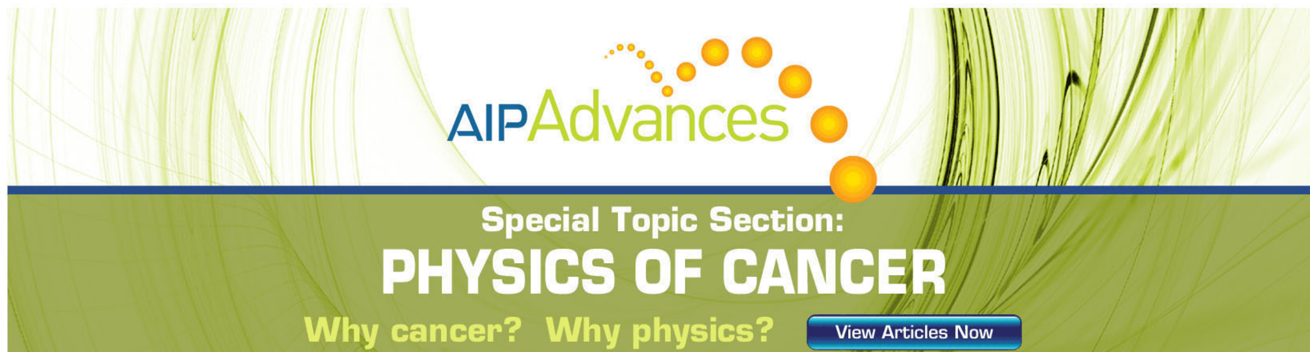

Downloaded 03 Jul 2012 to 77.236.37.84. Redistribution subject to AIP license or copyright; see http://apl.aip.org/about/rights_and_permissions

Shape control via surface reconstruction kinetics of droplet epitaxy nanostructures

C. Somaschini, S. Bietti, N. Koguchi, and S. Sanguinetti[a)]
L–NESS and Dip. di Scienza dei Materiali, Universitá di Milano Bicocca, Milano, Italy

(Received 1 August 2010; accepted 14 October 2010; published online 17 November 2010)

We present the fabrication and discuss the growth dynamics of two classes of GaAs quantum nanostructures fabricated by droplet epitaxy, namely, double rings and coupled ring-disks. Their morphological differences has been investigated and found to be originated by the kinetic of the changes in the surface reconstruction around the initially formed Ga droplets during the arsenization step. The control of surface reconstruction dynamics thus permits a fine tuning of the actual nanostructure shape at the nanoscale, based on pure self-assembling techniques. © *2010 American Institute of Physics*. [doi:10.1063/1.3511283]

Self-assembled quantum nanostructures (NSs) have been proposed and employed as active elements in quantum information technologies[1,2] and optoelectronics.[3,4] What makes quantum NS so attractive for these kind of applications is the ability to tune their optoelectronic properties by careful design of their size, composition, strain, and shape. These parameters set the confinement potential of electrons and holes, thus determining the electronic and optical properties of the quantum NS.[5,6] In fact, for the realization of NS-based devices the electronic properties and the coupling between quantum NSs should be freely accessible for engineering. During the last three decades molecular beam epitaxy (MBE) has been successfully applied for the fabrication of semiconductor quantum NSs, giving the possibility for the manipulation of nanocrystals size and shape at the nanoscale. By exploiting the self-organization in three dimensional nanometer sized clusters of semiconductor materials, it is therefore possible to achieve the desired level of control on the morphology of NSs. In this field, droplet epitaxy[7,8] (DE) has been shown as a key method for obtaining designable GaAs NSs with different shapes, such as quantum dots,[9] single[10] and multiple quantum rings,[11] quantum dots molecules,[12] and coupled ring-disks (RDs).[13] In DE, a III-column element molecular beam is initially supplied for the formation of droplets on the substrate surface and an As flux is subsequently used for the crystallization of droplets into the III-As NS. By a suitable selection of the growth conditions it is possible to carefully determine the final shape of the nanocrystals. In particular, ring shaped quantum NSs like double rings (RRs) or coupled RDs, two structures characterized by the presence of an inner ring encircled by an outer region with cylindrical symmetry, are of particular interest as high efficiency optoelectronic devices have been produced based on these NSs.[14,15] Even though these two systems are sharing the main morphological features, RRs and RDs can be clearly distinguished, since in the first case, a clear peak-and-valley line profile is present, while in the second case, a flat disk appears around the inner ring. Despite the high level of morphology control achieved in the DE fabrication of such ring shaped NSs, the mechanism which permits the differentiation between these two classes of NSs is not clarified yet. Here, we scan the growth parameter area where RRs and RDs fabrication has been reported[13,16–18] and, via detailed *in situ* and *ex situ* morphological characterizations, we identify the mechanism at the basis of the difference between the two structures. We show that the formation of a clear peak-and-valley height profile, typical of the RR structure, is related to the dynamics of the surface reconstruction around the Ga droplet during the arsenization step. In particular, the establishment and the subsequent ordering speed of the As-rich $c(4\times4)$ surface reconstruction around the Ga droplets during the crystallization process is the crucial ingredient for the differentiation between RRs and RDs.

The growth experiments were performed in a conventional GEN II MBE system equipped with an As valved cell on epiready semi-insulating GaAs (001) wafers. For every sample, just after the oxide desorption, we have grown a 500 nm thick buffer layer of GaAs and a 200 nm thick barrier layer of $Al_{0.3}Ga_{0.7}As$ at 580 °C. After that, the substrate temperature was decreased to 350 °C and the As pressure depleted until the background pressure in the growth chamber was below 1×10^{-9} Torr. Subsequently a Ga molecular beam equivalent to 6 MLs was supplied for the formation of droplets. During this step the surface reconstruction changed from the As-rich $c(4\times4)$ to the Ga-rich (4×6) and the appearance of a halo pattern confirmed the establishment of liquid droplets at the surface. At this point the experimental procedure followed for the crystallization of Ga droplets by As supply was different for each sample as follows: 4×10^{-7} Torr at 275 °C for Sample A; 4×10^{-7} Torr at 300 °C for Sample B; 4×10^{-7} Torr at 350 °C for Sample C, and 8×10^{-6} Torr at 350 °C for Sample D. In every sample the As irradiation was maintained for 10 min in order to ensure the complete crystallization. Reflection high energy electron diffraction (RHEED) was used as *in situ* probe during the growth. Surface morphology of the as-grown samples was investigated *ex situ* by means of atomic force microscopy (AFM).

Large area scans of the sample surface (not shown here) demonstrated that the density of the original gallium droplets (around 9×10^{8} cm^{-2}) nicely matches the density of the GaAs NSs in each sample, suggesting that every droplet is transformed into a GaAs nanocrystal at the end of the fabrication procedure. Figure 1 reports the AFM images of a single structure, one for each of the four fabricated samples. The NSs show a good cylindrical symmetry, with an outer

[a)]Electronic mail: stefano.sanguinetti@unimib.it.

 © 2010 American Institute of Physics

Downloaded 03 Jul 2012 to 77.236.37.84. Redistribution subject to AIP license or copyright; see http://apl.aip.org/about/rights_and_permissions

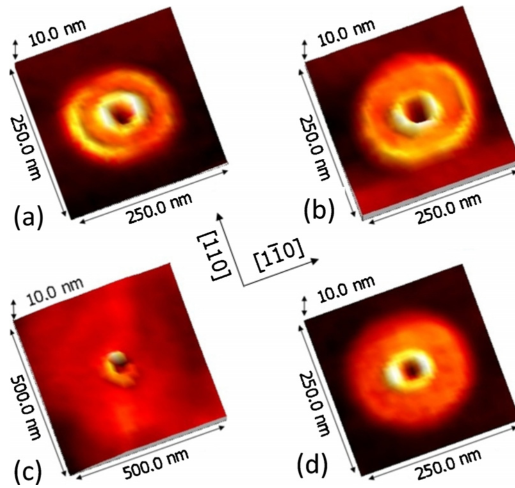

FIG. 1. (Color online) Magnified AFM images of the four presented samples. The crystallization conditions were: 4×10^{-7} Torr at 275 °C for Sample A, 4×10^{-7} Torr at 300 °C for Sample B, 4×10^{-7} Torr at 350 °C for Sample C, and 8×10^{-6} Torr at 350 °C for Sample D.

part which depends on the exact growth conditions and an inner ring, at the center of the NS, which displays the same radius irrespective of the sample preparation and which marks the original droplets position. We have recently shown that the inner ring in DE NSs is the result of the crystallization of Ga at the droplets edge, initiated by a partial dissolution of As inside liquid Ga, even in absence of intentional As supply.[11] On the contrary, the morphology of the outer circular regions, developed around the initially formed droplets, strongly depends on the crystallization conditions. A clear transition from the ringlike to the disklike geometry is observed as the growth temperature is increased. More detailed data on the evolution of the outer region can be derived from the cross sectional height profiles shown in Fig. 2. Comparing samples A, B, and C, it is evident that increasing the crystallization temperature results in the enlargement of the radius of the outer GaAs regions. The area of these regions depends on the surface diffusion coefficient of Ga atoms and is thus expected to increase with the temperature. In addition to this increase in the Ga diffusion length due to larger available thermal energy, more subtle morphology changes hap-

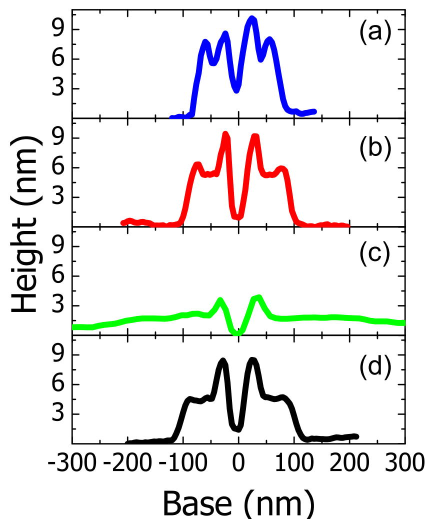

FIG. 2. (Color online) Cross-sectional height profiles along [1$\bar{1}$0] obtained from AFM data for Sample A (a), Sample B (b), Sample C (c), and Sample D (d).

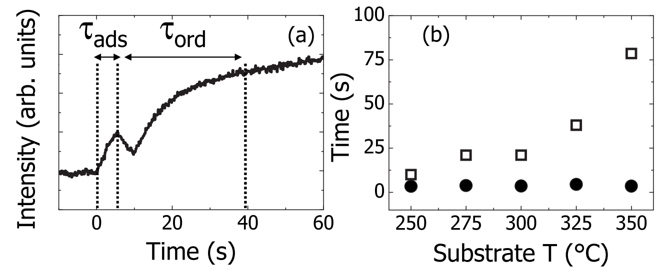

FIG. 3. Typical specular beam RHEED intensity change during As (4×10^{-7} Torr) adsorption on a droplets-free (4×6) reconstruction (a). τ_{ads} and τ_{ord} are indicated on the graph. Temperature dependence of τ_{ads} (circles) and τ_{ord} (squares) (b).

pen increasing the crystallization temperature. Indeed, the clear peak-and-valley profile shown by the lower growth temperature samples (A and B) is replaced at higher temperatures by a flat disk (samples C and D). Moreover, the shape transition between RR and RD cannot be attributed to the broadening of the diameter of the outer regions because Sample D, which has nearly the same diameter as Sample B, is instead characterized by the presence of a disklike outer region. It is worth noting that such deep change in NS morphology takes place in a rather narrow temperature window, between 300 °C and 350 °C. We are therefore in presence of a growth process rapidly changing with the temperature. In order to fully understand the observed behavior, we investigated the structural configuration of the substrate surface as it is seen by each Ga droplet during our growth experiments. Since RHEED can give only an information averaged over a relatively large area, we recorded the changes in the surface structure and the specular beam intensity as a function of time, during As adsorption on a dropletsfree (4×6) reconstruction. Figure 3(a) shows the typical specular beam intensity change during an As irradiation of 4×10^{-7} Torr beam equivalent pressure. Just after opening the As valve the specular beam increases, showing a maximum corresponding to the establishment of a (2×4) reconstruction, decreases and increases again after the initiation of a c(4×4) reconstruction which progressively orders until the specular beam intensity shows the saturation.[19] We define τ_{ads} as the time interval between the As cell opening and the formation of a (2×4) surface reconstruction and, in a similar way, τ_{ord} as the time interval between the establishment of the (2×4) and the ordering of the c(4×4). For the definition of τ_{ord} we take the point corresponding to $1-1/e^2$ times the saturation value of the specular beam intensity. In Fig. 3(b) the temperature dependence of τ_{ads} (circles) and τ_{ord} (squares) in the range used in our growth experiment is reported. It is worth noticing that the As flux and substrate temperatures used in these experiments for the As adsorption on a dropletsfree (4×6) reconstruction include exactly the same conditions employed in the fabrication of Samples A, B, and C. While in the first case τ_{ads} does not show any dependence on the temperature, τ_{ord} increases with increasing the substrate temperature. The process of adsorption of As atoms on the Ga-rich (4×6) until the formation of the As-stabilized (2×4), described by τ_{ads}, is therefore only dependent on the sticking of arsenic on the surface, which does not change with the temperature in the range 250–350 °C. On the contrary, the structural changes that are needed to transform the (2×4) into the c(4×4) show a temperature dependence, which

Downloaded 03 Jul 2012 to 77.236.37.84. Redistribution subject to AIP license or copyright; see http://apl.aip.org/about/rights_and_permissions

might also account for a different sticking coefficient of As atoms on the As-stabilized (2×4) reconstruction, in absence of Ga supply. These observations let us conclude that the appearance of $c(4\times4)$ regions is faster for lower substrate temperatures, like in the case of Sample A and B which showed a ringlike line profile.

The variation in the growth dynamics between the case of RRs and RDs can therefore arise from the different configuration of the substrate surface around the Ga droplets. Initially Ga droplets are sitting on the (4×6) surface reconstruction and, after the As supply, As adsorption promotes Ga atoms diffusion from the droplets. The size of the area covered by this diffusion is set by the average Ga migration distance which is determined by the diffusion coefficient and by the As adsorption time τ_{ads}, which is almost constant in our growth temperature range. At distances much larger than the Ga migration length, no Ga originated from the droplets can be found. In these areas the substrate surface will complete the transition to (2×4) and finally to the $c(4\times4)$ reconstruction, being the speed of this phenomenon, described by τ_{ord}, strongly dependent on the substrate temperature, as shown before. While Ga can easily diffuse on (2×4) surface, $c(4\times4)$ regions can act as preferential nucleation sites due to the large amount of As present on this As-rich configuration. Therefore the boundary of the $c(4\times4)$ region constitute a pinning point for Ga atoms diffusion. At lower temperatures, Ga atoms migrating from the droplet and reaching the border to the quickly formed $c(4\times4)$ region, will preferentially nucleate there and this phenomenon gives rise to the accumulation of GaAs at the distance from the droplets which marks the As rich region. This is what gives rise to the peak-and-valley line profile and it is what we normally call "outer ring." At higher temperatures, the establishment of the $c(4\times4)$ regions around the Ga droplets is a slow process and the crystallization of the available Ga atoms might finish before the formation of the As-rich regions. Ga atoms migrating from the droplets will not find any preferential site for the nucleation and thus will give rise to the disklike feature. In this case the lateral growth around the droplets will follow a real layer-by-layer mode, as we recently confirmed by the observation of the As-induced RHEED oscillations in similar systems.[13] Therefore the speed of the transition to the As-rich $c(4\times4)$ surface reconstruction plays a key role in determining the final shape of the DE NSs, meaning that the surface around the Ga droplets cannot be considered as inert during the crystallization process. For these reasons, the major changes in the NS shape between Sample B and C can now be fully explained. From one side, the larger diameter of Sample C is caused by the larger diffusion length of Ga atoms at higher substrate temperature, while from the other side, the absence of the peak-and-valley features that was present in Sample B is determined by the slower establishment of the $c(4\times4)$ reconstruction in the conditions of Sample C. In the case of Sample D, the high temperature used for the As supply caused the formation of a disklike outer zone, while the narrower diameter, compared to Sample C, appeared because of the shorter diffusion length of Ga atoms, in the case of higher As flux.[13] The nanoscale shape design of the NSs grown by DE is achievable through the control over the surface migration of Ga atoms and over the surface reconstruction changes during the As supply. Indeed, the diameter of the GaAs NSs as well as the actual shape of the outer region can be varied by setting the suitable substrate temperature and As flux used for the crystallization of the Ga droplets.

In conclusion, we show the crucial role of surface reconstruction kinetics in determining the DE NSs morphology. The effect of the As adsorption on the substrate surface reconstruction was investigated by RHEED, showing that the Ga stabilized (4×6) surface changes under As flux to the As stabilized (2×4) and then evolves to $c(4\times4)$ As-rich phase, after a structural reorganization. Fundamental for the control of shape in DE, the formation speed of As-rich $c(4\times4)$ regions is faster at lower temperatures. We analyzed in detail the formation of two classes of GaAs NSs, namely, RRs and RDs. These two systems share some main characteristics, like the presence of an inner ring at the center of the structure and a cylindrical outer region developed around the initially formed droplet. However the different shape of the outer portion of the NSs makes them clearly distinguishable, since a pronounced peak-and-valley height profile is present in the case of RRs, which are fabricated at lower substrate temperature. According to our observations, the protrusion which constitutes the outer ring in RR NS is formed because of the Ga preferential nucleation at the border of the As-rich $c(4\times4)$ regions, rapidly formed at low temperature. On the contrary at higher temperatures, when the speed of formation of an ordered $c(4\times4)$ is slower than the complete crystallization time of Ga atoms in the droplet, no preferential nucleation site is formed and a layer-by-layer growth mode takes place, giving rise to disklike features.

This work was supported by the CARIPLO Foundation under project QUADIS2 (Contract No. 2008-3186) and by the Italian PRIN-MIUR under project GOCCIA (Contract No. 2008CH5N34).

[1] G. Burkard, D. Loss, and D. P. DiVincenzo, Phys. Rev. B **59**, 2070 (1999).
[2] M. Bayer, P. Hawrylak, K. Hinzer, S. Fafard, M. Korkusinski, Z. Wasilewski, O. Stern, and A. Forchel, Science **291**, 451 (2001).
[3] Y. Arakawa and H. Sakaki, Appl. Phys. Lett. **40**, 939 (1982).
[4] V. Klimov, A. Mikhailovsky, S. Xu, A. Malko, J. Hollingsworth, C. Leatherdale, H. Eisler, and M. Bawendi, Science **290**, 314 (2000).
[5] W. Buhro and V. Colvin, Nature Mater. **2**, 138 (2003).
[6] J. Li and L. Wang, Nano Lett. **3**, 1357 (2003).
[7] N. Koguchi, S. Takahashi, and T. Chikyow, J. Cryst. Growth **111**, 688 (1991).
[8] N. Koguchi and K. Ishige, Jpn. J. Appl. Phys., Part 1 **32**, 2052 (1993).
[9] K. Watanabe, N. Koguchi, and Y. Gotoh, Jpn. J. Appl. Phys., Part 2 **39**, L79 (2000).
[10] T. Mano and N. Koguchi, J. Cryst. Growth **278**, 108 (2005).
[11] C. Somaschini, S. Bietti, N. Koguchi, and S. Sanguinetti, Nano Lett. **9**, 3419 (2009).
[12] M. Yamagiwa, T. Mano, T. Kuroda, T. Tateno, K. Sakoda, G. Kido, N. Koguchi, and F. Minami, Appl. Phys. Lett. **89**, 113115 (2006).
[13] C. Somaschini, S. Bietti, S. Sanguinetti, N. Koguchi, and A. Fedorov, Nanotechnology **21**, 125601 (2010).
[14] J. Wu, Z. Li, D. Shao, M. O. Manasreh, V. P. Kunets, Z. M. Wang, G. J. Salamo, and B. D. Weaver, Appl. Phys. Lett. **94**, 171102 (2009).
[15] J. Wu, D. Shao, Z. Li, M. O. Manasreh, V. Kunets, Z. Wang, and G. Salamo, Appl. Phys. Lett. **95**, 071908 (2009).
[16] T. Mano, T. Kuroda, S. Sanguinetti, T. Ochiai, T. Tateno, T. Kim, T. Noda, M. Kawabe, K. Sakoda, G. Kido, and N. Koguchi, Nano Lett. **5**, 425 (2005).
[17] S. Huang, Z. Niu, Z. Fang, H. Ni, Z. Gong, and J. Xia, Appl. Phys. Lett. **89**, 031921 (2006).
[18] J. Lee, Z. Wang, Z. Abuwaar, N. Strom, and G. Salamo, Nanotechnology **17**, 3973 (2006).
[19] C. Deparis and J. Massies, J. Cryst. Growth **108**, 157 (1991).

Downloaded 03 Jul 2012 to 77.236.37.84. Redistribution subject to AIP license or copyright; see http://apl.aip.org/about/rights_and_permissions